Separation Science and Technology
Publication details, including instructions for authors and subscription information:
http://www.informaworld.com/smpp/title~content=t713708471

CYPHOS IL 101 (Tetradecyl(Trihexyl)Phosphonium Chloride) Immobilized in Biopolymer Capsules for Hg(II) Recovery from HCl Solutions

E. Guibal[a]; K. Campos Gavilan[a]; P. Bunio[b]; T. Vincent[a]; A. Trochimczuk[b]
[a] Ecole des Mines Alès, Laboratoire Génie de l'Environnement Industrial, Alès cedex, France [b] Department of Chemistry, Technical University of Wrocław, Wrocław, Poland

To cite this Article Guibal, E. , Gavilan, K. Campos , Bunio, P. , Vincent, T. and Trochimczuk, A.(2008) 'CYPHOS IL 101 (Tetradecyl(Trihexyl)Phosphonium Chloride) Immobilized in Biopolymer Capsules for Hg(II) Recovery from HCl Solutions', Separation Science and Technology, 43: 9, 2406 — 2433

To link to this Article: DOI: 10.1080/01496390802118970

URL: http://dx.doi.org/10.1080/01496390802118970

Separation Science and Technology, 43: 2406–2433, 2008
Copyright © Taylor & Francis Group, LLC
ISSN: 0149-6395 print/1520-5754 online
DOI: 10.1080/01496390802118970

Taylor & Francis
Taylor & Francis Group

CYPHOS IL 101 (Tetradecyl(Trihexyl)Phosphonium Chloride) Immobilized in Biopolymer Capsules for Hg(II) Recovery from HCl Solutions

**E. Guibal,[1] K. Campos Gavilan,[1] P. Bunio,[2] T. Vincent,[1]
A. Trochimczuk[2]**
[1]Ecole des Mines Alès, Laboratoire Génie de l'Environnement Industrial,
Alès cedex, France
[2]Technical University of Wrocław, Department
of Chemistry, Wrocław, Poland

Abstract: A composite polymer (made of gelatin and alginate) was used for the synthesis of Cyphos IL 101-immobilized resins. These resins (with varying size and different ionic liquid (IL) content) have been tested for the recovery of mercury from concentrated HCl solutions (0.1–5 M HCl concentrations). Prior to the study of sorption performance on resins, the reactivity of Cyphos IL 101 versus mercury was tested using solvent extraction methodology. These results showed that the extraction was hardly affected by the concentration of HCl and that an ion exchange mechanism was probably involved in metal recovery (binding of $HgCl_4^{2-}$). The performance of these resins for Hg(II) recovery was tested through sorption isotherms and uptake kinetics, investigating the effect of resin size, ionic liquid content, metal concentration, agitation speed, and resin state (dry state versus wet state). Sorption capacity (which was proportional to the IL content) can reached up to 150 mg Hg g^{-1} in 1 M HCl; this sorption capacity was decreased by increasing chloride concentration. The kinetics were described well by the pseudo-second order equation and by the intraparticle diffusion equation (the so-called Crank's equation). The intraparticle diffusion coefficient was in the range of 10^{-11}–$1.2 \times 10^{-10}\,m^2\,min^{-1}$. The kinetic profiles were controlled by the IL content, sorbent dosage, and the sorbent particle size. Drying of the resins significantly decreased diffusion rates in the resins. The presence of competitor metals did not affect sorption capacity except when stable chloro-anionic species

Received 7 December 2007; accepted 7 April 2008.

Address correspondence to Eric Guibal, Ecole des Mines d'Alès Laboratoire Génie de l'Environnement Industrial Alex cedex, F-30319, France. E-mail: eric.guibal@ema.fr

such as in the case of Zn(II) were formed. Mercury can be desorbed using 6 M nitric acid solutions; and the sorbent can be recycled for at least six sorption/desorption cycles without significant decrease in the sorption performance.

Keywords: Cyphos IL 101, desorption, diffusion, immobilization, kinetics, mercury, sorption isotherm

INTRODUCTION

The stringent regulations concerning the discharge of wastewater to the environment have driven the interest of the research community toward the development of alternative processes for the recovery of organic and mineral contaminants. In the case of metal pollutants, a wide range of processes are offered for the removal of toxic metals, including precipitation, sorption onto resins or mineral sorbents (1–5), liquid-liquid extraction (6–8), or membrane processes (9,10). Mercury is recognized as a very dangerous metal, subject to natural accumulation in the food chain; for this reason the limitations for mercury discharge to the environment are becoming progressively more drastic. Precipitation is generally not selective (thus removal is more difficult to validate) and produces huge amounts of highly contaminated sludge (impossible to discharge without special conservative strategies). Membrane processes represent interesting alternatives; however, they face economical limitations in the case of large flow rates, especially in the case of reverse osmosis. In the case of ultrafiltration processes, the size of metal ions is not large enough to allow the metal to be retained, and the use of a macroligand is required for effectively recovering mercury. The binding of mercury ions to the macromolecule increases the size of mercury specie to a point where mercury is retained on the UF membrane; this is the basis of UFAC processes (ultrafiltration assisted by complexation) (9,10). Such membrane systems are frequently affected by fouling mechanisms that limit their long-time application. Wang et al. grafted mercapto groups on polysulfone membranes for mercury chelation (11). Solvent extraction is a widely used technology that faces several economical and environmental constraints due to the possible loss of extractant (environmental risk and costs) during the extraction process (7,8,12,13). For this reason a number of processes have been developed for immobilizing the extractant in the suitable matrix; this may be performed by impregnation, co-polymerization, or encapsulation steps. The immobilization can reduce the loss of extractant, and it makes possible the use of the system in simple fixed bed columns for commercial applications. The immobilization procedure usually consists in mixing the support with the extractant dissolved in a suitable solvent and then evaporating the solvent. The second process (i.e. more sophisticated) takes place during the synthesis of the resin. The third process, which was used in the present work, involves the encapsulation of the liquid extractant into a capsule made of polymer or biopolymers (14–19). A new class of solvents called ionic liquids has been developed by combining organic or inorganic cations and anions. Ionic liquids are noted for their low volatility. Among ionic liquids, the Cyphos family is a class of phosphonium derivatives (20), which was essentially developed for the purpose of immobilizing metals for catalytic applications (21–25), but are also useful for extraction purpose (26–28).

The present work investigates the sorption properties of Cyphos IL 101 immobilized into a composite biopolymer matrix for removing mercury from HCl solutions. Biopolymers are renewable resources; using such material for encapsulating IL makes the process interesting for sustainable growth. Additionally, these materials are easy to modify physically or chemically. The present work deals with resin particles but similar encapsulating procedures were carried out for conditioning flat membranes. A preliminary study is dedicated to the investigation of liquid-liquid extraction properties of the IL, including study of the effect of HCl concentration, metal concentration and IL concentration. In a second part of the study, the IL immobilized into the capsules is tested for Hg sorption in batch systems, with a special attention paid to the impact of HCl concentration, sorbent particle size, IL content into the capsules and metal concentration on the sorption capacity (including sorption isotherms). The kinetics of sorption are considered in a third part of the study investigating the impact of particle size, IL content, agitation speed, and metal concentration. The kinetic profiles are modeled using the pseudo-first order and pseudo-second order equations and the intraparticle diffusion model. Finally, the desorption of mercury from loaded resins is considered. Several eluents are tested, and the recycling of the resin is tested over 6 cycles.

MATERIALS AND METHODS

Materials

The Cyphos$^{®}$ IL 101 was kindly supplied by Cytec (Canada). This ionic liquid is a phosphonium salt (tetradecyl(trihexyl)phosphonium chloride, C.A.S. Number: [258864-54-9]). It is described as an ionic liquid that is slightly viscous at room temperature, immiscible with water and sparingly soluble in water; it dissolves water up to 8% (Cytec information). Its density decreases linearly with temperature (from 0.913 to 0.86 over the temperature range 0–90°C). Viscosity is highly dependent on the solute (water, hexane, etc.) and its concentration when dissolved in the Cyphos IL 101 (changing by 1 or 2 orders of magnitude when an organic solute is introduced). Viscosity decreases with temperature (by 3 orders of magnitude between -20°C and 100°C); by adjusting the temperature and/or the presence of an organic solute it is possible to give the ionic liquid a viscosity similar to water.

Alginate and gelatin were supplied by Acros Organics (Belgium). Other reagents (metal salts, NaCl, $NaNO_3$, mineral acids) were supplied as reagent grade products by Fluka AG (Switzerland).

Synthesis of Cyphos-Impregnated Capsules

The synthesis of the Cyphos-impregnated capsules was performed in 2 steps:

(a) 6.25 X g of Cyphos® IL 101 (previously mixed with 1.25 X g of a 10 M solution of NaOH) were mixed with 25 g of a 20% (w/w) aqueous solution of gelatin. Then 475–7.5 X g of alginate sodium solution (2% w/w) were added to the gelatin-ionic liquid solution and mixed under ultrasonic treatment until a slightly viscous white solution was obtained, with X = 1, 2, or 3 for respectively C1, C2 and C3 series.

(b) The composite solution was then extruded through a nozzle (internal diameter 0.6 mm) into an ionotropic gelling solution ($CaCl_2$, 6% in water, w/w).

The beads were maintained in the coagulation bath overnight before being rinsed with 0.1 M HCl solution. They were stored in 0.1 M HCl, in order to prevent possible degradation of the composite biopolymer matrix. The proportion of ionic liquid was modified to prepare resins with different IL content, changing the amount of gelatin and alginate according to the appropriate percentage required. Table 1 gives the main characteristics of the resins prepared by this procedure. Figure 1 shows the SEM photographs of three samples of resins, irregularly circular shapes are observed because the drying step introduced a little deformation of the beads.

Characterization of the resins was performed according to the following procedures. The water content of the resin was determined by weight loss at 60°C after 24 hours in an oven. Water regain was obtained by weight measurement of dry beads that were wetted in 0.1 M HCl solution overnight. The size of particles was determined by

Table 1. Resins characteristics

Resin	Diameter (wet, mm)	Diameter (dry, μm)	Cyphos content (%, d.w.)	Cyphos content (mmol/g d.w.)	Water content (%)(a)	Water regain (%)(a)
C1S	1.00 ± 0.04	435 ± 80	35.9 ± 1.3	0.692	84/81	11/43
C1L	2.33 ± 0.02	988 ± 74	31.4 ± 0.6	0.604	90/81	15/51
C2S	0.85 ± 0.06	472 ± 75	50.3 ± 0.9	0.968	76/ND	15/40
C2L	2.67 ± 0.03	1313 ± 48	44.6 ± 0.9	0.860	88/82	12/29
C3L	2.58 ± 0.02	1600 ± 51	57.3 ± 1.8	1.103	86/80	ND/31

(*a*): first number shows data for oven drying; second number shows data for air drying.

ND: not determined.

measurement of the beads on photographs and measurement from retro-projection of the beads. Ionic liquid content was determined by phosphorus analysis using ICP-AES (inductively coupled plasma atomic emission spectrometry, JY 2000, Jobin-Yvon, Longjumeau, France) after chemical degradation of the polymer matrix. A known amount (50–100 mg depending on IL content) was mixed with 2 mL of sulfuric acid and heated till complete mineralization occurred (destruction of polymer capsule). After cooling, 1 mL of hydrogen peroxide was added drop by drop. The mixture was heated until bubbles disappeared and discoloration was complete. After cooling and volumetric adjustment, the P content was measured to evaluate the molar IL concentration in the resin.

Liquid-Liquid Experiments

Preliminary evaluations of the affinity of Cyphos IL 101 for Hg were performed through liquid-liquid experiments. The objective of this part

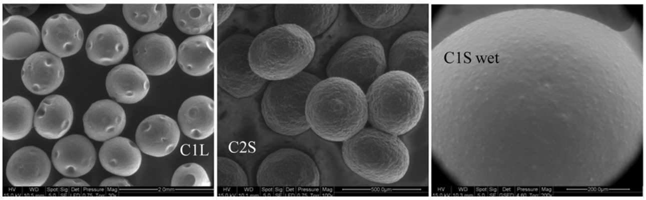

Figure 1. Scanning electron microscopy of C1L and C2S sorbent particles (dry state) and C1S (wet state, environmental scanning electron microscope).

of the work was not a thorough study of liquid-liquid extraction properties of Cyphos IL 101 for Hg, but it focused on the preliminary evaluation of the impact of main experimental parameters on Hg recovery. The IL was dissolved in either hexane or toluene at concentrations ranging between 1 mM and 125 mM. The mixture was mixed with an equal volume of an aqueous mercury solution (1 g Hg L^{-1}) prepared from HCl solutions (with concentrations ranging between 0.1 and 5 M). The solutions were shaken in a reciprocal shaker for 1 hour and, the residual metal concentration was measured after settling in the aqueous phase for establishing the extraction yield and the distribution coefficient. When the formation of a third phase or other problems were observed in the aqueous solution, a drop of methanol (or alternatively KNO_3) was added to the mixture before separating the aqueous and organic phases; this was sufficient for separating clear phases. The distribution ratio, D, is defined as the ratio $Hg(II)_{org}/Hg(II)_{aq}$ (ratio of concentrations of the solute in the organic and aqueous phases).

Sorption and Desorption Experiments

The experimental procedure was carried out in several steps to evaluate

(a) influence of environmental parameters (concentration of HCl, Cl^-, NO_3^-, competitor metals...) and intrinsic resin characteristics (IL content) on equilibrium sorption;
(b) impact of selected parameters (HCl concentration) on sorption isotherms;
(c) influence of resin state (drying procedure) and metal concentration on uptake kinetics;
(d) desorption (and resin recycling).

To evaluate equilibrium performance, a volume of acid solution (30 mL in most cases) containing the appropriate concentration of Hg was mixed with a known amount of resin (i.e. 20 mg). The slurry was agitated for 96 hours to be sure equilibrium was reached. The residual concentration of Hg was measured by ICP-AES analysis after filtration. The sorption loading (q, mg Hg g^{-1} or mmol Hg g^{-1}) was determined by the mass balance equation: $q = V(Co\text{-}C_{eq})/m$, where Co and C_{eq} are the initial and equilibrium concentrations (mg Hg L^{-1} or mmol Hg L^{-1}) of Hg, respectively; V is the volume of solution (L); and m the mass of resin (g). The distribution ratio, D, is defined as the ratio of sorption (mercury loading) to residual metal concentration $D = q/C_{eq}$, L g^{-1}. To investigate the influence of competitor ions, sodium chloride and sodium nitrate were added to the initial solution as salts, and $CuCl_2$, $NiCl_2$, $ZnCl_2$, and $CdCl_2$ salts were added to the solution to examine the effect of competitor metals.

Sorption isotherms were obtained by mixing fixed amounts of resin (i.e. 20 mg) with fixed volumes (i.e. 100 mL) of HCl solutions of increasing concentrations (0.1 M, 1 M, and 2 M), containing Hg concentrations in the range 20 to 200 mg Hg L^{-1}). At equilibrium (i.e. after 96 hours of contact), the residual concentration was used to calculate the sorption (Hg loading).

Uptake kinetics were investigated by adding, under agitation, a known amount of resin (i.e. 200 mg, dry weight, in most case except when investigating the impact of sorbent dosage) to 1 L of Hg (Co: 10–100 mg Hg L^{-1}) solutions prepared in 1 M HCl solutions. Low sorbent dosage has been selected in order to detect the contribution of intraparticle diffusion resistance, which has been shown to be a limiting step in these materials (15). Samples were collected, filtered, and analyzed at fixed times.

Desorption was performed by mixing loaded sorbent (about 20 mg, with known concentration of mercury) with a known volume of eluent (nitric acid, thiourea, and potassium iodide in acidic media) for fixed times. The amount of mercury released was used for calculating Hg desorption yield. For the study of resin recycling, a rinsing step was carried out, using a 0.1 M HCl solution, before using the resin for the next adsorption step. The amount of Hg bound to the resin and subsequently desorbed was obtained by the mass balance equation for the sorption and elution steps, respectively. Comparison of these values enabled the desorption yield (%) to be calculated.

Characterization of Resins by SEM-EDAX

Element distribution (especially Hg and P, as the tracer of Cyphos IL 101) in the beads was investigated by Environmental Scanning Electron Microscopy (ESEM) Quanta FEG 200, equipped with an OXFORD Inca 350 Energy Dispersive X-ray microanalysis (EDX) system. The system can be used to acquire qualitative or quantitative spot analyses and qualitative or quantitative X-ray elemental maps and line scans. This ESEM allows samples to be analyzed at pressures and humidity which approach normal laboratory conditions and avoids experimental artifact. More specifically, with this system it is possible to analyze the samples at much higher pressure than with conventional SEM. Alternatively dry samples of free or saturated extractant-encapsulated beads were embedded in synthetic resin EPOTEK 301:4 parts glue and 1 part lubricant. After a drying step of 24 h at mild temperature, the embedded beads were cut, and sections were polished with a series of abrasive GEOPOL disks of decreasing grain size (6/12, 2/6, and 0.5/3 mm). The sections were rinsed with water between each pair of abrasive disks after the polishing step. Finally the sections were polished with a fine tissue using a DP emulsion lubricant (DP lubricant) and diamond spray HQ (successive sizes 6, 3, and 1 mm). Finally, the sections were coated with carbon or gold by metallization (to increase sample conductivity), when necessary.

RESULTS AND DISCUSSION

Liquid-Liquid Extraction

The preliminary investigation of the affinity of Cyphos IL 101 for Hg(II) was performed with liquid-liquid extraction technique using hexane and toluene as solvent of the IL. Under selected experimental conditions (i.e. Co: 1 g Hg L^{-1}, ca. 5 mmol L^{-1}), the extraction efficiency increased with IL content up to 10 mmol L^{-1}, corresponding to the complete recovery of the metal. The stoichiometric ratios IL/Hg(II) for the full removal of the metal tended to 2:1. The study of the distribution of Hg(II) species in 1 M HCl solutions reveals that the predominant species is $HgCl_4^{2-}$ (about 95%, remaining species is $HgCl_3^{-}$). These observations lead to the conclusion that Hg(II) is probably extracted by an ion exchange mechanism involving two molecules of IL per molecule of chloroanionic mercury species. Figure 2 also shows that the concentration of HCl had a negligible impact on Hg(II) extraction efficiency in the range 0.1–2 M, and only a limited effect when the HCl concentration was raised to 5 M. The profiles were not affected by the kind of solvent used.

The weak effect of HCl concentration is confirmed on Fig. 3 (a) and (b) by the superimposition of the distribution curve for Hg(II) versus the concentration of Cyphos IL 101. For IL concentrations higher than 0.25, the distribution ratio tended to correlate linearly (in the log-log plot) with IL concentration. Hexane diluent seems to give slightly better Hg(II) extraction than toluene. This is confirmed by Fig. 3 (c) and (d) that show the distribution ratio (in the log-log plot) versus residual Hg(II) concentration. The values of the distribution ratios were generally slightly higher with hexane and the plots were generally shifted toward higher concentrations of IL for toluene solvent.

Characterization of Cyphos IL 101 Immobilized Resins

SEM-EDAX analysis was performed on resins embedded in epoxy resins (cut and polish sections) to evaluate the distribution of elements in the resin before and after Hg sorption for all resin samples (selected analyses

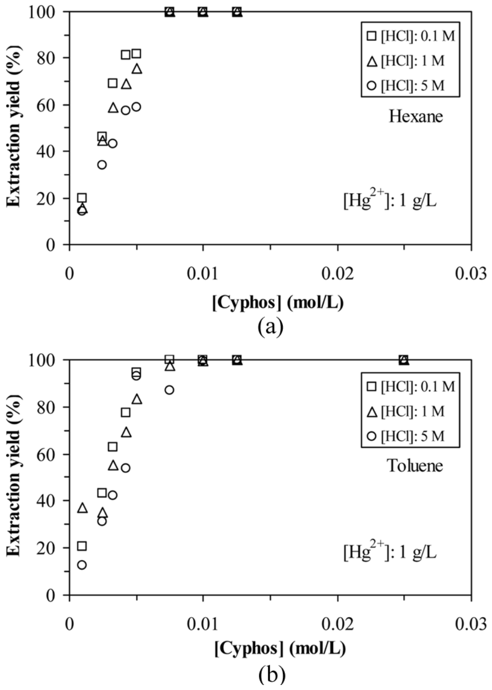

(a)

(b)

Figure 2. Influence of Cyphos IL 101 concentration and HCl concentration on Hg(II) extraction (solvent: hexane or toluene).

are presented below). For raw beads the distribution of P was followed as a tracer of the distribution of Cyphos IL 101 in the resin (homogeneity of the resin bead), and for Hg(II)-loaded resins both P and Hg element were analyzed. Figure 4 shows the case of C2S resin after Hg loading. The cartography of Hg and P distribution and the concentration profile of these elements along a central cross-section confirm

(a) that the IL was uniformly distributed in the whole resin, and
(b) that Hg was also distributed in the whole mass of the resin. This means that the sorbent can be fully saturated and that all the reactive groups remained accessible.

Figure 5 shows the case of large resin particles with high IL content (C3L) partially loaded with mercury. While the raw resin (before metal binding) showed a homogeneous distribution of IL in the whole mass (constant profile of P along a cross-section), after Hg sorption the profiles of P and Hg distribution indicate that P density (and thus IL)

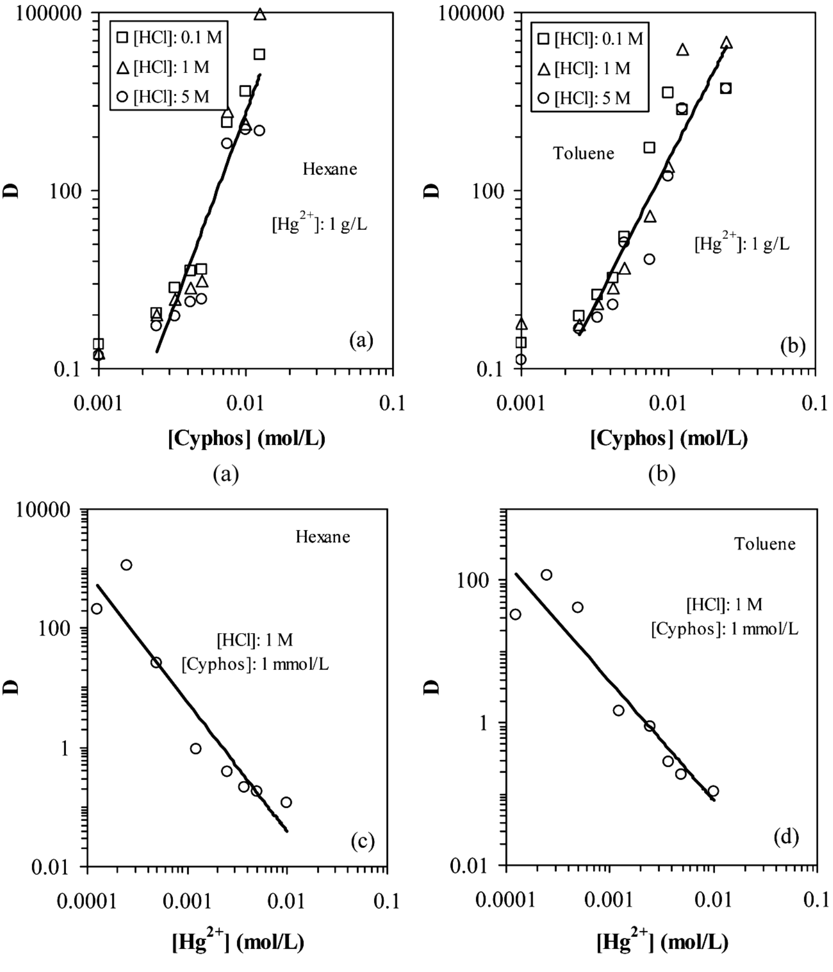

(a) (b)

(c) (d)

Figure 3. Influence of Cyphos IL 101 concentration (a and b) and Hg(II) concentration (c and d) on Hg(II) distribution ratio from 1 M HCl solutions in hexane and toluene solvent.

was less in the central part of the resin and that Hg was almost not sorbed at the center of the particle. The absence of Hg in the center of the resin was expectable since the resin was not metal-saturated. Complementary experiment with Hg-saturated resin showed that Hg was present in the whole mass of the resin (not shown). The absence of mercury at the center of the particle in the course of the sorption process confirmed that the sorption process took place through a shrinking core mechanism, which

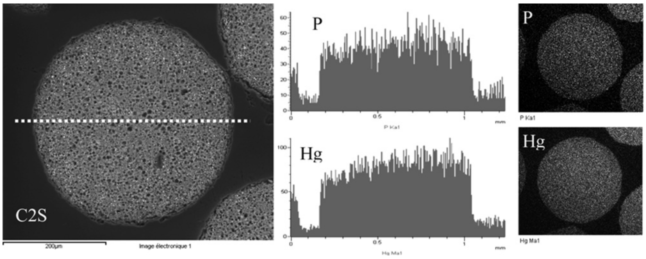

Figure 4. SEM microphotograph, distribution of elements (P, representative of Cyphos IL 101 distribution, and Hg) along a cross-section (line) and cartography of element distribution for C2S resin after saturation.

is probably controlled by diffusion. It is surprising to observe that during the sorption process P distribution was not homogeneous in the whole mass of the resin (contrary to the original distribution). This could indicate that the IL was not tightly bound to the matrix and that the interaction of the IL with metal ions contributed to IL migration and aggregation phenomena at the shrinking core layer.

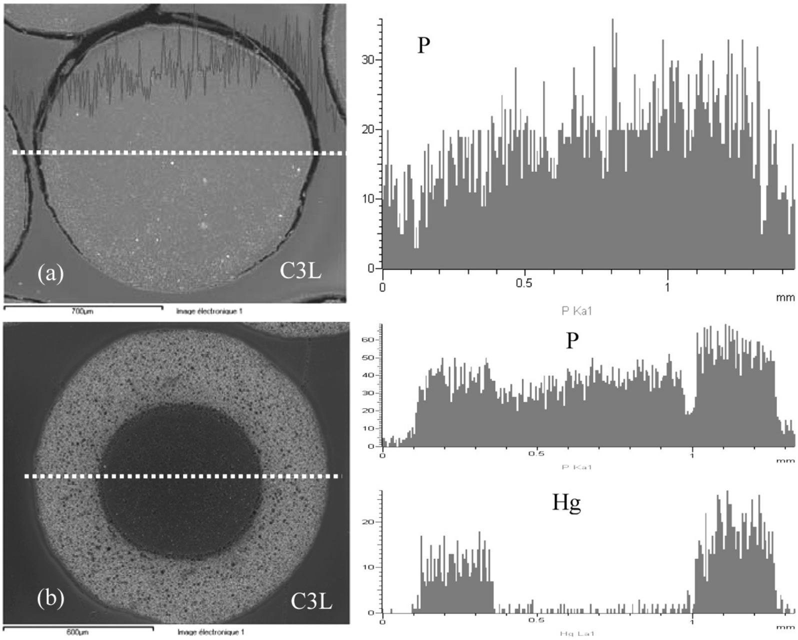

Figure 5. SEM, and distribution of elements (P and Hg) through a cross-section (line) for C3L resin before (a) and after (b) Hg binding.

Influence of HCl Concentration and Cl⁻ Concentration

Experiments have been performed at different initial concentrations (i.e. 120 and 200 mg Hg L^{-1}) with two lots of resins (C2S and C2L) for investigating the impact of HCl concentration and that of chloride concentration (at low HCl concentration, i.e. 0.1 M) on sorption capacity (Fig. 6). The increase of HCl concentration decreased sorption capacity by 20–30% when increasing the concentration of HCl from 0.1 to 2 M; above 2 M the variation was less significant. Similar trends were observed with 0.1 M HCl solutions completed by addition of NaCl to reach total chloride concentrations comparable to those set for the study of HCl effect. Metal speciation was calculated using the Medusa Software and the equilibrium constants (29):

$$Hg^{2+} + i\ Cl^{-} \leftrightarrow HgCl_i^{2-i} \tag{1}$$

With log K$_i$: 6.75, 13.12, 14.03 and 14,44 for i: 1–4, respectively.

At low Cl$^-$ concentration (i.e. 0.1 M), $HgCl_4^{2-}$ represents about 46% of total Hg(II) species (31% for $HgCl_2$ and 23% for $HgCl_3^-$). When increasing total Cl$^-$ concentration (under either HCl or NaCl form) the fraction of

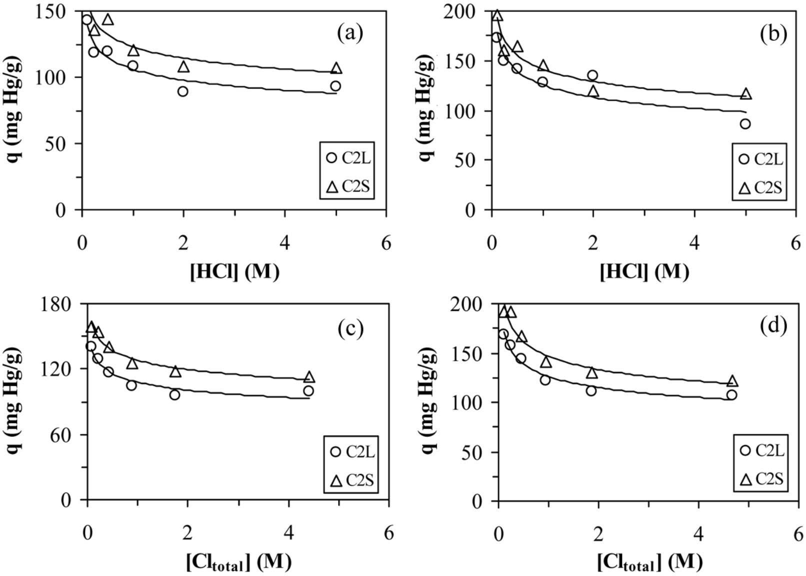

Figure 6. Influence of HCl concentration (a and b) and NaCl concentration (for 0.1 M HCl solutions; (c and d) on Hg(II) sorption capacity (Co(Hg): 120 mg L^{-1}–(a and c); Co(Hg): 200 mg L^{-1}–(b and d) (SD: 20 mg resin/30 mL solution).

$HgCl_4^{2-}$ increases up to 68% (for [Cl^-]: 0.2 M), 80% (for [Cl^-]: 0.3 M) and 90% (for [Cl^-]: 0.5 M). This means that there is no direct correlation between sorption performance and the predominance of $HgCl_4^{2-}$; sorption loading results from a compromise between the presence of favorable species (chloroanionic mercury species, and more specifically $HgCl_4^{2-}$) and the competition effect of chloride ions. The acidity of the solution did not play an important role in the impact of chloride ions since the decrease in sorption capacity did not appear to be significantly different for the experimental series involving [HCl] and [Cl^-]$_{tot}$ variations.

Sorption Isotherms

Sorption isotherms have been established for 1 M HCl solutions for the different series of resins (Fig. 7(a)). The isotherms were characterized

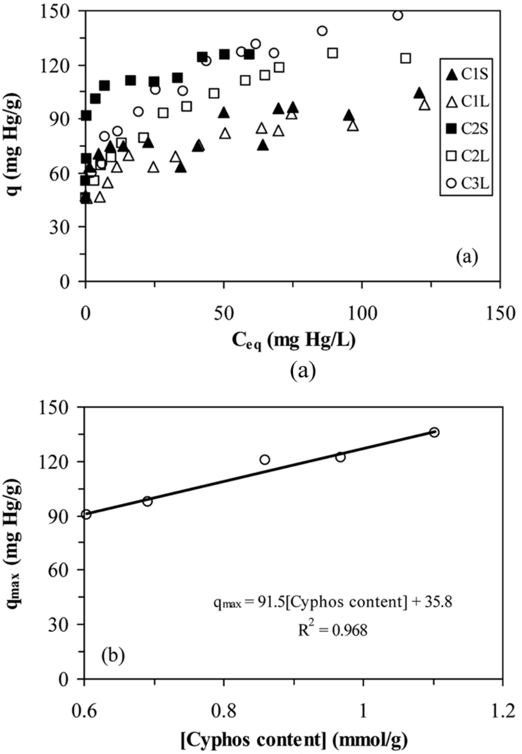

(a)

(b)

Figure 7. Hg(II) sorption isotherms for the different resins (a), and correlation between maximum sorption (q_{max}) and Cyphos IL 101 content in the resins (b).

by steep initial slopes followed by a plateau appearing at low residual metal concentration. This trend is typical of most irreversible equations. The formation of a plateau means that the isotherm will be better described by the Langmuir equation than by the Freundlich equation. However, the steep curvature suggests that the fit will not be very good; indeed the Langmuir equation assumes a progressive increase of the sorption capacity that is not compatible with the rectangular shape of the experimental isotherms. Applying the Langmuir equation (not shown) gave correlation coefficients in the range 0.96–0.99, with affinity coefficients that did not vary regularly in function of the IL content of the resin due to the difficulty to fit the experimental curvature of the isotherms. This is the reason for not discussing these Langmuir parameters. More interesting is the discussion of the maximum sorption capacities calculated as the average value of the last experimental points on the plateau of each isotherm. The maximum sorption capacity (q_{max}) was plotted versus IL content in the resin (Fig. 7b). The plot showed a linear correlation between q_{max} and Cyphos IL 101 content. Based on molar units, the correlation relationship gives a stoichiometric ratio Hg(II)/Cyphos IL 101 close to 0.46, which is consistent with the suggested mechanism involving two Cyphos IL 101 molecule for the binding of one Hg(II) molecule. The size of the sorbent particle does not seem to play an active role; this was expectable since this parameter is expected to mostly influence diffusion mechanism. It may affect the time required to reach equilibrium rather than the equilibrium value. Actually Fig. 7b shows that the maximum sorption capacity was proportional to IL content. This means that even in the case of high IL loading, all the reactive groups may be accessible at long reaction time, independently of the modifications of the gel structure observed on Fig. 5.

Cieszyńska et al. investigated the liquid/liquid extraction of Pd(II) from HCl solutions using Cyphos IL-101 (30). They suggested several mechanisms depending on the concentration (and speciation of HCl). At low HCl concentration (i.e. 0.1 M), Pd(II) is suspected to be extracted under the form $R_3R'P^+ \cdot PdCl_3^-$; while at high HCl concentration (i.e. 3 M HCl), the binding involves $(R_3R'P^+)_2 \cdot PdCl_4^{2-}$. Most of the experiments performed in the present study were carried out in 1 M HCl solutions, which correspond to the predominance of $HgCl_4^{2-}$. This is consistent with the suspected mechanism involving the interaction of 2 molecules of IL per molecule of anionic chlorocomplex of mercury, corresponding to the stoichiometry obtained at saturation of the different resins.

Sorption Kinetics

The sorption kinetics may be controlled by various diffusion mechanisms:

(a) bulk diffusion,
(b) film diffusion, and
(c) intraparticle diffusion.

Additionally, the chemical reaction can play a significant role in the control of the kinetics. In the experimental series, a very low solid/liquid ratio (i.e. 200 mg L^{-1}, in most cases) was intentionally selected to prevent the sorption from being limited to surface sites and to show evidence of contribution of intraparticle diffusion. This means also that the time required to reach equilibrium (typically 72 h) may appear longer than for systems involving much greater sorbent dosages.

Three models were used for the description of kinetic profiles based on the pseudo-first order and the pseudo second-order equation described by Ho (31), and on the intraparticle diffusion equation defined by Crank (32).

Pseudo first-order equation (the so-called Lagergren equation):

$$\log(q_e - q_t) = \log q_e - \frac{k_1}{2.303}\mathrm{t} \tag{2}$$

Where q_e is the amount of metal ion sorbed at equilibrium (mg Hg g^{-1}); q_t is the amount of metal sorbed (mg Hg g^{-1}) at any time, t; and k_1 is the pseudo-first order rate constant (min^{-1}). The parameters q_e and k_1 are pseudo-constants to be determined by linear regression on the linear segment of the experimental curves.

$$\text{Pseudo second} - \text{order equation :} \qquad \mathrm{q_t} = \frac{q_\infty^2 \times k_2 \mathrm{t}}{1 + q_\infty \times k_2 \mathrm{t}} \tag{3}$$

Where k_2 is the pseudo-second-order rate constant (g mg^{-1} min^{-1}). The parameters q_∞ and k_2 are pseudo-constants, depending on experimental conditions; they were obtained after linearization of the equation to:

$$\frac{\mathrm{t}}{\mathrm{q_t}} = \frac{1}{k_2 q_\infty^2} + \frac{1}{q_\infty}\mathrm{t} \tag{4}$$

The intraparticle diffusion coefficient (D_e, effective diffusivity, m^2 s^{-1}) was determined using Crank's equation which assumes the solid to be initially free of metal and that the external diffusion resistance is not limiting, especially after long contact time (32):

$$\frac{q(t)}{q_{eq}} = 1 - \sum_{n=1}^{\infty} \frac{6\alpha(\alpha+1)\exp\left(\frac{-D_e q_n^2 t}{r^2}\right)}{9 + 9\alpha + q_n^2\alpha^2} \tag{5}$$

In this equation, q(t) and q_{eq} are the concentrations of the metal in the resin at time and equilibrium respectively; r is the radius of resin particles.

And q_n are the non-zero roots of the equation:

$$\tan q_n = \frac{3\ q_n}{3 + \alpha q_n^2} \tag{6}$$

$$\text{with } \frac{q_{eq}}{VC_o} = \frac{1}{1+\alpha} \tag{7}$$

Tables 2–4 summarize the parameters for the different models applied to the different experimental series. In most cases the comparison of the

Table 2. Modeling of sorption kinetics–Pseudo-first order equation

Resin	v (rpm)	Co (mg Hg L^{-1})	SD (g L^{-1})	Sorbent state	q_e (mg Hg g^{-1})	k_1*10^3 (min^{-1})	R^2
C1S	500	50	0.2	Dry	74.2	3.34	0.992
C1L	500	10	0.2	Dry	35.4	0.82	0.973
C1L	500	25	0.2	Dry	52.8	0.76	0.978
C1L	500	50	0.2	Dry	61.7	0.87	0.971
C2S	300	50	0.2	Dry	87.2	1.38	0.965
C2S	500	50	0.2	Dry	104.7	2.19	0.984
C2S	300	35	0.2	Dry	88.5	1.40	0.966
C2S	300	100	0.2	Dry	118.1	4.10	0.968
C2L	300	20	0.2	Dry	58.3	0.66	0.979
C2L	300	50	0.2	Dry	77.0	0.71	0.975
C2L	300	80	0.2	Dry	87.1	0.78	0.973
C2L	300	30	0.2	Dry	70.8	0.70	0.988
C2L	300	30	0.3	Dry	62.5	0.74	0.991
C2L	300	30	0.4	Dry	56.0	0.86	0.989
C2L	500	50	0.2	Dry	85.4	0.80	0.937
C3L	300	20	0.2	Dry	63.9	0.74	0.988
C3L	300	50	0.2	Dry	88.8	0.64	0.975
C3L	300	80	0.2	Dry	102.7	0.68	0.969
C3L	500	50	0.2	Dry	76.6	0.78	0.983
C3L	500	50	0.2	Wet	100.8	1.77	0.988

Table 3. Modeling of sorption kinetics–Pseudo-second order equation

Resin	v (rpm)	Co (mg Hg L^{-1})	SD (g L^{-1})	Sorbent state	q_∞ (mg Hg g^{-1})	$k_2{}^{*}10^5$ (g mg^{-1} min^{-1})	R^2
C1S	500	50	0.2	Dry	87.8	9.2	0.999
C1L	500	10	0.2	Dry	38.8	5.2	0.950
C1L	500	25	0.2	Dry	62.0	5.8	0.982
C1L	500	50	0.2	Dry	70.2	6.3	0.971
C2S	300	50	0.2	Dry	122.0	7.1	0.996
C2S	500	50	0.2	Dry	123.9	5.0	0.997
C2S	300	35	0.2	Dry	116.1	5.6	0.997
C2S	300	100	0.2	Dry	141.7	8.3	0.998
C2L	300	20	0.2	Dry	61.1	4.0	0.965
C2L	300	50	0.2	Dry	81.3	3.6	0.943
C2L	300	80	0.2	Dry	97.0	2.8	0.967
C2L	300	30	0.2	Dry	80.6	3.2	0.965
C2L	300	30	0.3	Dry	71.4	4.4	0.970
C2L	300	30	0.4	Dry	65.2	4.7	0.986
C2L	500	50	0.2	Dry	100.2	2.8	0.986
C3L	300	20	0.2	Dry	75.7	1.9	0.972
C3L	300	50	0.2	Dry	95.2	2.0	0.936
C3L	300	80	0.2	Dry	117.1	1.6	0.959
C3L	500	50	0.2	Dry	88.7	3.9	0.978
C3L	500	50	0.2	Wet	118.6	4.4	0.994

experimental data with predictions from equations (2) and (4) shows that the pseudo-second order equation fit the experimental data better than the pseudo-first order equation. Additionally, the comparison of the equilibrium sorption loadings (q_e and q_∞) calculated with the models described by Equations (2) and (4) with the corresponding experimental values also showed a better correlation when using the pseudo-second order equation.

Influence of Agitation Speed

The agitation speed is one of the experimental parameters that can be checked for evaluating the contribution of film diffusion on the control of kinetics. The kinetic profiles were compared under the same experimental conditions changing agitation speed from 300 to 500 rpm (not shown). The differences were not very marked. The tables confirm that the agitation speed (in the range 300–500 rpm) did not affect mass transfer; the intraparticle diffusion coefficient varied by less than 8% when increasing the agitation speed. This is less than the variation in the

Table 4. Modeling of sorption kinetics–Intraparticle diffusion

Resin	v (rpm)	Co (mg Hg L^{-1})	SD (g L^{-1})	Sorbent state	D_e*10^{11} (m^2 min^{-1})
C1S	500	50	0.2	Dry	3.0
C1L	500	10	0.2	Dry	1.4
C1L	500	25	0.2	Dry	4.0
C1L	500	50	0.2	Dry	5.0
C2S	300	50	0.2	Dry	2.3–2.5
C2S	500	50	0.2	Dry	2.2
C2S	300	35	0.2	Dry	1.4
C2S	300	100	0.2	Dry	4.0
C2L	300	20	0.2	Dry	3.8
C2L	300	50	0.2	Dry	7.5–8.3
C2L	300	80	0.2	Dry	8.3
C2L	300	30	0.2	Dry	5.0
C2L	300	30	0.3	Dry	3.9
C2L	300	30	0.4	Dry	2.1
C2L	500	50	0.2	Dry	8.5
C3L	300	20	0.2	Dry	5.0
C3L	300	50	0.2	Dry	9.5
C3L	300	80	0.2	Dry	10.8
C3L	500	50	0.2	Dry	12.5
C3L	500	50	0.2	Wet	52.0

repeatability of the experiments. The variations observed for the pseudo-second order equation were not very large as pointed out on Tables 2 and 3. This is a first indication that film diffusion is not the limiting mechanism for Hg(II) sorption.

Influence of Sorbent Dosage

Increasing the amount of sorbent, increased the density of sorption sites, which in turn decreased the residual concentration at equilibrium (Fig. 8). With a sorbent dosage of 400 mg L^{-1}, 90% of mercury was removed. Tables 2–4 show that the sorption capacity at equilibrium logically decreased when increasing the sorbent dosage. The rate parameter (both k_1 and k_2) increased with the sorbent dosage, while the intraparticle diffusion coefficient decreased slightly (remaining in the range 2×10^{-11} to $5 \times 10^{-11}\, m^2\, min^{-1}$). Increasing the sorbent dosage resulted in an increase in interfacial surface and a greater initial slope of the curve; the gradient of concentration between the surface and the center of the particle decreased, inducing a decrease of the calculated intraparticle diffusion coefficient.

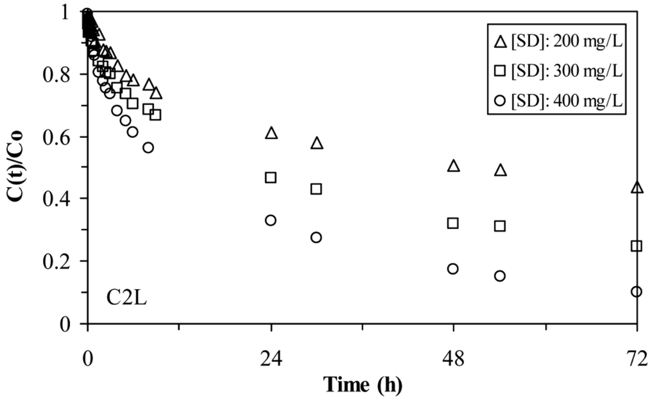

Figure 8. Influence of sorbent dosage on Hg(II) sorption kinetics using C2L resin (Co: 50 mg Hg L^{-1}; v: 300 rpm, [HCl]: 1 M).

Influence of Particle Size and IL Content

The five resins were compared under the same experimental conditions; though the IL content of the resins changed for the different lots, the direct comparison will be difficult since the sorption capacity changed with the IL content. Figure 9 shows that the smallest particles reached faster the equilibrium; 30–32 hours were sufficient for reaching the equilibrium while more than 70 hours were required for the largest particles. For small beads, increasing IL content did not change significantly the intraparticle diffusion coefficient (decreasing from 3.0×10^{-11} $m^2\,min^{-1}$ to 2.2×10^{-11}

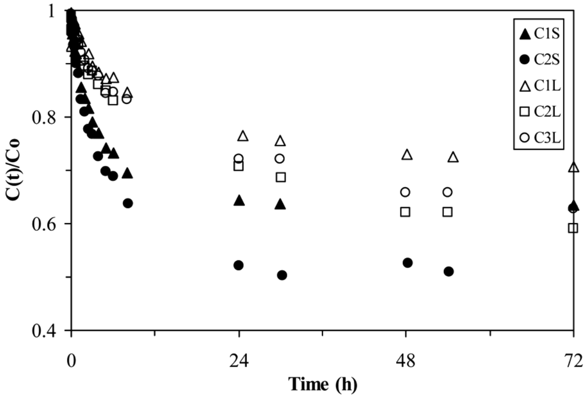

Figure 9. Influence of Cyphos IL 101 content and particle size on Hg(II) sorption kinetics ([SD]: 200 mg L^{-1}; Co: 50 mg Hg L^{-1}; v: 500 rpm; [HCl]: 1 M).

$m^2\,min^{-1}$). In the case of large bead, the intraparticle diffusion coefficient increased linearly with IL content. For a given IL content, the intraparticle diffusion coefficient increased with the size of the particles. For the pseudo-second order equation the variations of the constants of the model did not follow a regular linear trend. It is possible to conclude that both IL content and particle size have significant impact on the profile of sorption kinetics and on intraparticle diffusion, but the impact is especially important for large particles. It is not possible to separate the effects of particle size and IL content; these parameters have crossed impact.

Influence of Initial Hg(II) Concentration

The influence of metal concentration was tested on kinetic profiles for two sizes of resins prepared with comparable IL contents (ca. 0.962 mmol IL g^{-1} for C2S and 0.86 mmol IL g^{-1} for C2L). Figure 10 reports the results obtained with different initial concentrations. As expected, the smallest particles reached equilibrium earlier than for largest particles. The intraparticle diffusion coefficient increased with the initial concentration of mercury in the solution, probably due to a higher concentration gradient between the outlet of the resin and the inlet concentration. These diffusion coefficients were systematically greater for large particles compared to small particles. The variation of the intraparticle diffusion with the size of the beads may be explained by different IL content and by possible differences in the distribution of IL materials. As expected, increasing the initial concentration increased the sorption capacity at equilibrium in the modeling of the pseudo-second order equation. The conclusion is a bit more complex when considering the rate parameter (i.e. k_2). With small particle size, the rate parameter increased

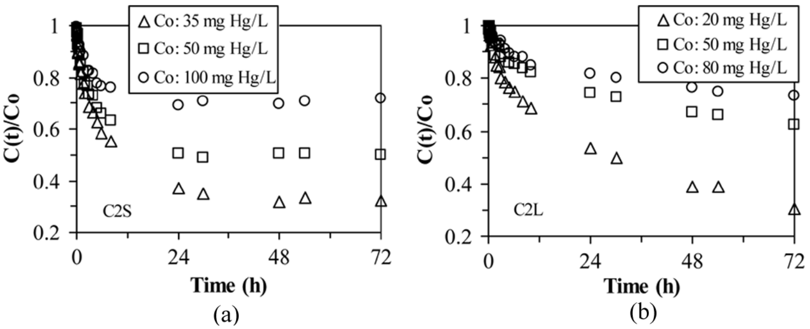

(a) (b)

Figure 10. Influence of initial Hg(II) concentration on Hg(II) sorption kinetics for C2S and C2L resins ([SD]: 200 mg L^{-1}; v: 300 rpm; [HCl]: 1 M).

with increasing metal concentration while a reciprocal trend was observed for large resin particles. However, for both small and large particles the variation was generally limited to 25–30% for the extreme values.

Influence of Drying Step

The drying of the resin results in a partially irreversible shrinking of resin particles. The large water content in wet resin beads made the reproducibility of the experiments difficult. Additionally, the wet resins (though stored in acidic media) were not perfectly stable at long storage time. For these reasons, investigation of the sorption properties of dry resins was preferred. However, taking into account the strong contribution of intraparticle diffusion in the control of kinetics, it appeared interesting to do a limited number of experiments with wet resins. Indeed, the irreversible shrinking of biopolymer gels generally affects intraparticle diffusion (33). Figure 11 shows the comparison of kinetic profiles for wet (raw) resins and dried resins. The sorption capacity decreased after drying as evidenced by the significantly higher values of residual Hg(II) concentration. The initial slope of the kinetics was also considerably increased when using wet resins. This effect was reinforced at using large particles (C3L). The rate parameter for the pseudo-second order equation was not significantly affected by the drying treatment (varying from 4.4 to 3.9 g mg^{-1} min^{-1}). The impact was significantly greater for the intraparticle diffusion coefficient that decreased by a factor 4 when drying the resin. This result confirms the drastic impact of the irreversible shrinking of the resin occurring under drying operations.

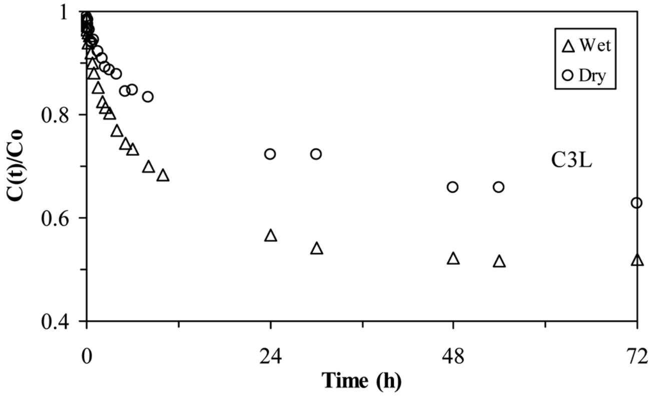

Figure 11. Influence of the drying of the resin (C3L) on Hg(II) sorption kinetics (Co: 50 mg Hg L^{-1}; [SD]: 200 mg L^{-1}; v: 500 rpm; [HCl]: 1 M).

Influence of Competitor Ions

The effect of the presence of increasing concentrations of competitor base metals (Zn(II), Ni(II) and Cu(II)) has been tested on Hg(II) sorption using C2L resin (Fig. 12). In the range 100–1000 mg L^{-1} of competing ions (for a 100 mg Hg L^{-1} concentration), the sorption capacity was not significantly affected; the sorption capacity remained in the range 110–120 mg Hg g^{-1}. When the concentration increased to 5 g L^{-1}, the impact of the competing ions became significant; the sorption capacity decreased to 100 mg Hg g^{-1} for Cu(II) and Ni(II). This decrease in sorption capacity probably can be explained by the competing effect of the counter ion (present in the salt added to the mercury solution, i.e. chloride ions). At a concentration of metal close to 5 g L^{-1}, the amount of chloride added represents an increase in the concentration of the anion close to 0.2 M. This additional concentration of chloride anions probably contributed more to the competitor effect of metal ions than their direct effect since these metals do not form stable chloro-anions under selected experimental conditions, and they cannot be bound to Cyphos IL 101 with the suggested interaction mechanism. This was confirmed by the weak variation of the concentration of the competitor ions (less than 2%, this means close to the detection limit, taking into account dilution and analytical limits). The behavior of Zn(II) is different since this metal can form stable chloro-anions in HCl solutions. In 1 M HCl solutions five different Zn(II) species may coexist: Zn^{2+} (26%), $ZnCl^{+}$ (24%), $ZnCl_2$ (16%), $ZnCl_3^{-}$ (18%)

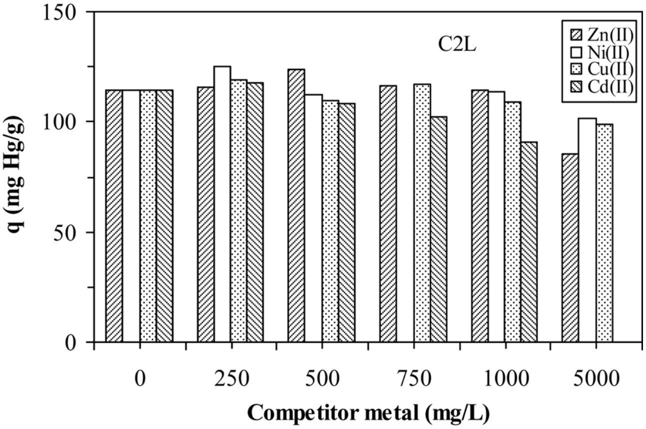

Figure 12. Influence of increasing concentrations of competitor ions (Zn(II), Ni(II), Cu(II) and Cd(II)) on Hg(II) sorption in 1 M HCl solutions using C2L resin (V: 100 mL; m: 20 mg; Co: 100 mg Hg L^{-1}; contact time: 96 h).

and $ZnCl_4^{2-}$ (16%). The impact of chloride ions was not detectable at concentrations in the range 0.1–1 g Zn L^{-1}; at the highest concentration (i.e. 5 g Zn L^{-1}), the sorption capacity decreased to 85 mg Hg g^{-1}. This diminution of the sorption capacity can probably be explained by the combined competitor effects of chloride anions and zinc chloro-anions. Similar results were obtained in the presence of increasing concentrations of cadmium, probably due to the formation of chloro-anionic cadmium species. In 1 M HCl solutions, Cd(II) is present in three forms: $CdCl^+$ (19%), $CdCl_2$ (49%) and $CdCl_3^-$ (32%). The impact was stronger for Cd(II) compared to Zn(II); in the presence of Cd(II) at the concentration of 1 g L^{-1} the sorption capacity was close to 90 mg Hg g^{-1} while it remained close to 112 mg Hg g^{-1} in the presence of other metals (Zn(II), Cu(II), Ni(II) at 1 g metal L^{-1}). Based on these preliminary results on competition effects, the affinity of the resin for these metals can be ranked according: Hg(II) > Cd(II) > Zn(II). These results confirm that the resins are selective for the metals forming anionic species in HCl solutions.

The influences of competing anions have been tested through the effect of chloride anions addition (Fig. 6 (c) and (d)). The influence of nitrate anions was also tested by adding increasing concentrations of sodium nitrate (up to 5 g L^{-1}). Under selected experimental conditions ([HCl]: 0.1 M; m/V: 200 mg L^{-1}; [Hg^{2+}]: 100 mg L^{-1}), the sorption capacity remained close to the reference value (nitrate-free solution, not shown); the sorption capacity varied by less than 4% around 182 mg Hg g^{-1} in the range (0–5 g NO_3^- L^{-1}). Though the experimental conditions were not the same as for chloride anions solutions, the impact of nitrate seems to be less marked compared to chloride anions and to metal chloro-anions.

Desorption

Several eluents were tested in order to remove Hg(II) from loaded resins; the best results were obtained with concentrated nitric acid (6 M), potassium iodide (1 M) and thiourea (1 M). Due to the weak stability of the resin in alkaline media, KI and thiourea were tested in HCl solutions (1 M). Figure 13 shows the kinetic profiles for the desorption of Hg(II)-loaded C2L resin using these eluents. Eluents can be ranked according to their desorption yield: Nitric acid (97%) > Thiourea (80%) > KI (20%). This figure also shows that 2 hours of contact were sufficient for reaching the desorption equilibrium; this means that the desorption mechanism was much faster than the sorption process. This is probably due to the difference in the diffusion properties of the eluent and the eluted species.

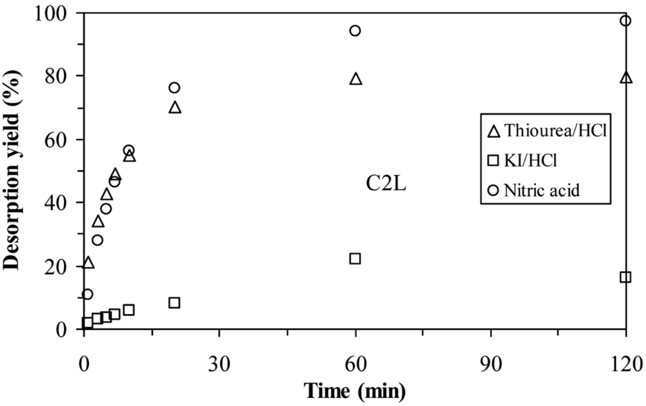

Figure 13. Hg(II) desorption kinetics for C2L resin loaded in 1 M HCl solutions (100 mL of 70 mg Hg L^{-1} solution, 20 mg of resin) using molar solutions of KI and thiourea (in 1 M HCl solutions) and HNO_3 (6 M) (100 mL of eluent, 20 mg of resin).

The Crank's equation (Equation (4)), coupled with Equations (5) and (6) can be used for desorption (32), providing the Equation (6) is changed to:

$$\frac{3M^r_\infty}{n\ 4\pi r^3 C'_o} = \frac{1}{1+\alpha} \tag{8}$$

where M^r_∞ is the amount of solute released at equilibrium and C'_o is the concentration of the solute in the resin. The symbol n is the number of resin beads (4/3 πr^3, representing the volume of a single sphere). The left-hand term represents the desorption yield at equilibrium. This equation has been tested for simulating the desorption profile of Hg(II) from C2L. The intraparticle diffusion coefficient was $3.5 \times 10^{-10}\,m^2\,min^{-1}$. This means five to ten times greater than the values reached for sorption isotherms (Table 4).

Six sorption/desorption cycles were operated on C3L resin using 6 M nitric acid and 1 M thiourea (in 1 M HCl solutions) for the desorption step. The results are summarized in Figure 14. They confirm that nitric acid is the most appropriate eluent for Hg(II) recovery from loaded resin. The sorption capacity remained almost constant over the six cycles, and the desorption (though not complete) also remained at a high level over the six cycles. The comparison of the total amount of mercury adsorbed and desorbed on the six cycles showed that the desorption yield was close to 87% for nitric acid and close to 79% for thiourea. Actually, 10 to 20% of mercury remained in the resin

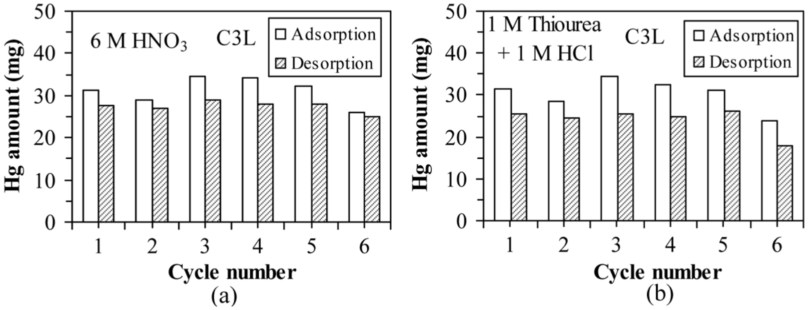

Figure 14. Influence of agitation speed on Hg(II) sorption kinetics (Co: 50 mg Hg L^{-1}; [SD]: 200 mg L^{-1}, [HCl]: 1 M).

after 6 sorption/desorption cycles. Though no physical evidence can be observed, it is possible to suggest that a kind of condensation of Hg-IL compounds within the pores of the resin had occurred making the metal less accessible to desorption agent.

CONCLUSION

Cyphos IL 101 was successfully immobilized in a composite of biopolymers (gelatin to make the IL compatible with the encapsulating media and alginate as the shape-forming material). Several resins were prepared with different size and different IL content. These resins are stable in acidic solution (even in concentrations as high 5 M HCl) but are not appropriate for operating at neutral or alkaline pH.

These resins can bind metal-forming anionic species in acidic solutions (such as chloro-anions). In the case of Hg(II) sorption, capacities as high as 150–200 mg Hg(II) were obtained even in 1 M HCl solutions. The mechanism involved in metal binding is an anion exchange mechanism involving the binding of $HgCl_4^{2-}$. Increasing the concentration of chloride ions (in an acidic form or a salt form) decreased the sorption loading, though sorption capacities as high as 80–100 mg Hg g^{-1} were maintained at 5 M chloride concentration under selected conditions (this means a 30% decrease compared to the 0.1 M chloride concentration). The sorption capacity linearly increased with IL content; the stoichiometric ratio confirmed extraction of Hg(II) through the form $(IL^{+})_2 \cdot HgCl_4^{2-}$. The kinetic profiles were well described by the pseudo-second order equation and by the intraparticle diffusion equation (the so-called Crank's equation). The weak effect of the agitation speed (in the range 300–500 rpm) confirmed the limited impact of film diffusion resistance on the control of sorption kinetics. Increasing the size of resin particles increased the time of contact required for reaching the equilibrium. The most important parameters for controlling the kinetic profiles are the sorbent dosage, the IL content in the resin, the concentration of mercury and the drying state of the resin. Intraparticle diffusivity coefficient remained in the range 10^{-11} to $1.2 \times 10^{-10}\,m^2\,min^{-1}$ for selected experimental conditions, but this coefficient significantly increased when the resin was used under the wet form (value increased from 1.2×10^{-10} to $5 \times 10^{-10}\,m^2\,min^{-1}$). The presence of competitor metal did not significantly affect Hg(II) sorption, except when the competitor metal forms stable chloro-anionic species under selected experimental conditions (for example Zn(II) or Cd(II)). However, even in large excess of such a competitor metal the sorption capacity did not decrease by more than 30%. Mercury loaded on the resin can be readily desorbed by nitric acid preferentially to thiourea (in 1 M HCl solution) with kinetic rates that were faster than for sorption steps. The resins were operated over six sorption/desorption cycles maintaining high level of metal recovery and with a cumulative desorption yield that was close to 87%.

ACKNOWLEDGMENTS

Authors thank Erasmus program (from European Union) and La Region Languedoc Roussillon for supporting the visit of P. Bunio at Ecole des Mines Alès. Authors (E.G. and T. V.) also acknowledged Carnot Program support for the "Encapsulation" Project. Authors thank Alain Diaz and Jean-Marie Taulemesse from the Centre des Matériaux de Grande Diffusion (Ecole des Mines Alès) for the preparation of polished sections and the SEM-EDAX analysis of samples. Authors also thank Dr. Al Robertson (Cytec, Canada) for providing Cyphos IL 101 sample.

REFERENCES

1. Arica, M.Y.; Bayramoglu, G.; Yilmaz, M.; Bektas, S.; Genc, O. (2004) Biosorption of Hg^{2+}, Cd^{2+}, and Zn^{2+} by Ca-alginate and immobilized wood-rotting fungus. *Funalia trogii. J. Hazard. Mater.*, *109* (1–3): 191.
2. Jeon, C.; Höll, W.H. (2003) Chemical modification of chitosan and equilibrium study for mercury ion removal. *Water Res.*, *37* (19): 4770.
3. Kacar, Y.; Arpa, C.; Tan, S.; Denizli, A.; Genc, O.; Arica, M.Y. (2002) Biosorption of Hg(II) and Cd(II) from aqueous solutions: comparison of

biosorptive capacity of alginate and immobilized live and heat inactivated. *Phanerochaete Chrysosporium. Process Biochem.*, *37* (6): 601.

4. Kawamura, Y.; Yoshida, H.; Asai, S.; Tanibe, H. (1998) Recovery of $HgCl_2$ using polyaminated highly porous chitosan beads - Effect of salt and acid. *J. Chem. Eng. Jpn.*, *31* (1): 1.
5. Pazirandeh, M. (1996) Development of a metallothionein based heavy metal biosorbent. *Biochem. Mol. Biol. Int.*, *39* (4): 789.
6. Duche, S.N.; Pawar, S.D.; Dhadke, P.M. (2002) Comparative study for extraction of Hg(II) with cyanex-923 from chloride and bromide media and its separation from Cd(II) and Zn(II). *Sep. Sci. Technol.*, *37* (9): 2215.
7. Francis, T.; Reddy, M.L.P. (2002) Radiochemical extraction of mercury(II) from acidic chloride solutions using dialkylsulphides. *J. Radioanal. Nucl. Chem.*, *252* (1): 99.
8. Meera, R.; Francis, T.; Reddy, M.L.P. (2001) Studies on the liquid-liquid extraction of mercury(II) from acidic chloride solutions using Cyanex 923. *Hydrometallurgy*, *61* (2): 93.
9. Barron-Zambrano, J.; Laborie, S.; Viers, P.; Rakib, M.; Durand, G. (2002) Mercury removal from aqueous solutions by complexation-ultrafiltration. *Desalination*, *144*: 201.
10. Kuncoro, E.K.; Roussy, J.; Guibal, E. (2005) Mercury recovery by polymer-enhanced ultrafiltration: comparison of chitosan and poly(ethylenimine) used as macro-ligand. *Sep. Sci. Technol.*, *40* (1–3): 659.
11. Wang, B.; Yang, X.L.; Huang, W.Q. (2007) Preparation and recovery of polysulfone affinity membrane with mercapto as chelating group for Hg^{2+} cations. *J. Appl. Polym. Sci.*, *103* (4): 2514.
12. Francis, T.; Rao, T.P.; Reddy, M.L.P. (2000) Cyanex 471X as extractant for the recovery of Hg(II) from industrial wastes. *Hydrometallurgy*, *57* (3): 263.
13. Francis, T.; Reddy, M.L.P. (2003) Thiosubstituted organophosphinic acids as selective extractants for mercury(II) from acidic chloride solutions. *Solvent Extr. Ion Exch.*, *21* (1): 109.
14. Fournel, L.; Navarro, R.; Saucedo, I.; Guibal, E. (2001) Cadmium Extraction with Cyanex 302-impregnated Chitosan Beads. In: *Biohydrometallurgy: Fundamentals, Technology and Sustainable Development (IBS 2001)*, Ciminelli, V.S.T.; Garcia, O.; jr., eds.; Elsevier: Amsterdam (The Netherlands), 109.
15. Guibal, E.; Vincent, T. (2006) Palladium recovery from dilute effluents using biopolymer-encapsulated extractant. *Sep. Sci. Technol.*, *41* (11): 2533.
16. Mimura, H.; Ohta, H.; Akiba, K.; Onodera, Y. (2001) Selective uptake and recovery of palladium by biopolymer microcapsules enclosing Cyanex 302 extractant. *J. Nucl. Sci. Technol.*, *38* (5): 342.
17. Mimura, H.; Ohta, H.; Hoshi, H.; Akiba, K.; Onodera, Y. (2001) Uptake properties of palladium for biopolymer microcapsules enclosing Cyanex 302 extractant. *Sep. Sci. Technol.*, *36* (1): 31.
18. Ngomsik, A.-F.; Bee, A.; Siaugue, J.-M.; Cabuil, V.; Cote, G. (2006) Nickel adsorption by magnetic alginate microcapsules containing an extractant. *Water Res.*, *40* (9): 1848.

19. Outokesh, M.; Mimura, H.; Niibori, Y.; Tanaka, K. (2006) Equilibrium and kinetics of silver uptake by multinuclear alginate microcapsules comprising an ion exchanger matrix and Cyanex 302 organophosphinic acid extractant. *Ind. Eng. Chem. Res.*, *45* (10): 3633.
20. Del Sesto, R.E.; Corley, C.; Robertson, A.; Wilkes, J.S. (2005) Tetraalkylphosphonium-based ionic liquids. *J. Organometal. Chem.*, *690* (10): 2536.
21. Wong, H.T.; Pink, C.J.; Ferreira, F.C.; Livingston, A.G. (2006) Recovery and reuse of ionic liquids and palladium catalyst for Suzuki reactions using organic solvent nanofiltration. *Green Chem.*, *8* (4): 373.
22. Gerritsma, D.A.; Robertson, A.; McNulty, J.; Capretta, A. (2004) Heck reactions of aryl halides in phosphonium salt ionic liquids: library screening and applications. *Tetrahedr. Lett.*, *45* (41): 7629.
23. Datta, A.; Ebert, K.; Plenio, H. (2003) Nanofiltration for homogeneous catalysis separation: soluble polymer-supported palladium catalysts for Heck, Sonogashira, and Suzuki coupling of aryl halides. *Organometallics*, *22* (23): 4685.
24. Hon, Y.S.; Lee, C.F.; Chen, R.J.; Szu, P.H. (2001) Acetonyltriphenylphosphonium bromide and its polymer-supported analogues as catalysts in protection and deprotection of alcohols as alkyl vinyl ethers. *Tetrahedron*, *57* (28): 5991.
25. Parvulescu, V.; Popa, A.; Davidescu, C.M.; Valceanu, R.; Vass, M.; Luca, C. (1997) Phase-transfer catalytic activity of polymer-supported ammonium and phosphonium salts in oxidation of benzyl alcohol with hydrogen peroxide. *React. Funct. Polym.*, *33* (2–3): 329.
26. Martak, J.; Schlosser, S. (2007) Extraction of lactic acid by phosphonium ionic liquids. *Sep. Purif. Meth.*, *57*(3): 483.
27. Regel-Rosocka, M.; Cieszynska, K.; Wisniewski, M. (2006) Extraction of zinc(II) with selected phosphonium ionic liquids. *Przemysl Chemiczny*, *85* (8–9): 651.
28. Martak, J.; Schlosser, S. (2006) Phosphonium ionic liquids as new, reactive extractants of lactic acid. *Chemical Papers-Chemicke Zvesti*, *60* (5): 395.
29. Puigdomenech, I. (2002) MEDUSA (Make equilibrium diagrams using sophisticated algorithms), v. 3.1, accessed: February 7, 2007, Royal Institute of Technology, Stockholm, Sweden, http://www.kemi.kth.se/medusa.
30. Ciezynska, A.; Regel-Rosocka, M.; Wisniewski, M. (2007) Extraction of palladium(II) ions from chloride solutions with phosphonium ionic liquid Cyphos IL101. *Pol. J. Chem. Technol.*, *9* (2): 99.
31. Ho, Y.S. (2006) Second-order kinetic model for the sorption of cadmium onto tree fern: a comparison of linear and non-linear methods. *Wat. Res.*, *40* (1): 119.
32. Crank, J. (1975) *The Mathematics of Diffusion*; Oxford University Press: Oxford, U.K., p. 414.
33. Ruiz, M.A.; Sastre, A.M.; Guibal, E. (2002) Pd and Pt recovery using chitosan gel beads: I. Influence of drying process on diffusion properties. *Sep. Sci. Technol.*, *37* (9): 2143.